FFEMS Fatigue & Fracture of Engineering Materials & Structures
ORIGINAL CONTRIBUTION
doi: 10.1111/ffe.12263

Fatigue behaviour of clinched joints in a steel sheet

J-B. KIM and H-K. KIM

Department of Mechanical and Automotive Engineering, Seoul National University of Science and Technology, Seoul National 172 Kongrung-dong, Nowon-ku, Seoul, 139-743, Korea

Received Date: 22 April 2014; Accepted Date: 20 October 2014; Published Online: 19 December 2014

ABSTRACT Clinch joining has been used in sheet metal work owing to its simplicity and because it facilitates the joining dissimilar metal sheets. In this study, monotonic and fatigue tests were conducted using coach-peel and cross-tension type specimens to evaluate the fatigue strength of clinch joints in a cold-rolled mild steel sheet. The monotonic experimental results reveal that the coach-peel specimen exhibits the lowest monotonic strength among the three specimen configurations. The coach-peel and cross-tension specimen geometries exhibit very low fatigue ratios, compared with the tensile-shear specimen. The maximum von Mises and principal stresses at the fatigue endurance limit are much higher than the engineering tensile strengths of the steel sheet used to determine the three specimen geometries. Compared with the effective stress and maximum principal stress, the Smith–Watson–Topper fatigue parameter can be used for an appropriate prediction of the current experimental fatigue life. With regard to the coach-peel specimen geometry, all samples exhibit pull-out failure mode in the fatigue testing range. However, for the cross-tension specimen geometry, mixed (pull-out and interface) and interface failure modes occurred, depending on the number of cycles to failure.

Keywords clinch joints; coach-peel; cold-rolled steel sheet; cross-tension; fatigue life.

NOMENCLATURE

BD	= button diameter
CT	= cap thickness
E	= young modulus
h	= height
N_f	= number of cycle to failure
NT	= neck thickness
p_{amp}	= load amplitude
PD	= punch diameter
R	= load ratio
SPCC	= steel plate cold commercial
SWT	= Smith-Watson-Topper fatigue parameter
t_1	= punch side metal thickness
t_2	= die side metal thickness
σ'_f, ε'_f, c,b	= material constants
$\Delta\varepsilon_1/2$	= maximum principal strain amplitude
$\sigma_1^{\max}$	= maximum stress on the $\Delta\varepsilon_1$ plane

INTRODUCTION

Spot welding has been the dominant means of fastening sheets of steel for automotive applications. Increased use of aluminium and magnesium alloys to lower the weights of vehicles has limited the use of spot welding in automotive applications. Clinch joining has been used in sheet metal work because of its simplicity and because it allows the joining of dissimilar sheet metals, such as steel, aluminium and magnesium alloy sheets. Another advantage of clinch joining in production is that it does not generate poisonous gas. Moreover, it is a relatively quiet process, and it requires low energy consumption.[1]

Correspondence: H-K. Kim. E-mail: kimhk@seoultech.ac.kr

Clinch joining is a combination of drawing and forming to lock together layers of sheet metal without the use of additional elements. During clinch joining, a punch drives the two layers of metal into a die with a grooved bottom perimeter that produces an impression. Additional force spreads the upper layer of material into the lower layer. Thus, the upper layer cannot be pulled out of the bottom layer. The joint is similar to a button.

Despite the fact that clinch joining is widely used, nearly all previous studies in this area have focused on monotonic joints and the related joining process.[2–5] Davies *et al.*[2] investigated the shear strength of clinch joints, taking into consideration the effects of the sheet thickness, loading angle and the ultimate tensile strength on the peak load and failure mode. Varis and Lepisto[3] proposed a parameter that they termed X to evaluate the quality of a clinch joint. This parameter is calculated based on the material volumes on the punch and die sides. When the die is completely filled, the clinch joint is optimized with a maximum volume of material in the region of the joint neck and a minimum value of the X parameter, leading to a tight joint. Paula *et al.*[4] conducted a finite element method (FEM) analysis of the joining process while varying the punch and die geometry. They suggested that the introduction of protrusions at the punch corners leads to higher joint strength. Hamel *et al.*[5] argued that an explicit FEM analysis is a fast and efficient numerical method with which to study the influence of tool geometry on the final joint geometry during the clinch joining process for the optimization of the joint strength.

The fatigue performance and failure mechanisms of clinch joints are not well established. Experimental investigations are necessary to generate more information on their fatigue performance levels. However, only a limited number of studies have been conducted on the fatigue behaviour of clinch joints. For example, Carboni *et al.*[6] investigated the static and fatigue behaviour of clinch joints using tensile-shear specimen geometry for a steel sheet. They conducted a FEM analysis of the specimen geometry while adopting linear-elastic deformation behaviour, reporting that the value of the fatigue endurance limit is close to half that of the ultimate joint strength. They determined that the fatigue life was a function of load amplitude instead of using a stress term and argued, based on FEM, that the failure site coincides with the location with the highest stress concentration. Recently, Kim[7] investigated the fatigue strength of clinch joints using tensile-shear specimen geometry for a steel sheet. That study reported that the fatigue limit approached 43% of the maximum tensile load at a load ratio of 0.1. They also reported that the maximum von Mises stress is very close to the ultimate tensile strength of the steel sheet based on FEM analysis results at the fatigue endurance limit. This implies that the true tensile strength of the neck is significantly increased through cold clinch joining.

To evaluate the fatigue strength of clinch joints, the applied load amplitude-life (ΔP-N_f) curve is widely used as a convenient method. However, the fatigue life of a clinch joint specimen is governed by several factors, including the load magnitude, loading type and specimen geometries. One of the problems commonly associated with fatigue life predictions of various clinch joint geometries has been the need to test each type of geometry. Even for the same button diameter, sheet material and sheet thickness, the fatigue strength in terms of either the maximum load or the load range can differ from one specimen type to another. To address this problem, stress-based approaches are needed for fatigue predictions of these joints.

Therefore, in this study, monotonic and fatigue tests were conducted using coach-peel and cross-tension specimens of a cold-rolled mild Steel Plate Cold Commercial (SPCC) sheet. The fatigue life of clinch joint specimens was evaluated, and several prediction parameters pertaining to the fatigue lifetimes of these joints were adopted. Finally, an appropriate parameter for predicting the fatigue lifetimes of coach-peel and cross-tension specimens was proposed, including those of the tensile-shear geometry discussed in other work by this author.[7]

EXPERIMENTAL PROCEDURES

Specimen preparation

Cold-rolled mild steel with a thickness of 0.8 mm was used in this study. The tensile properties of the steel were measured on a universal testing machine (Instron 8516, England). The engineering stress–strain curve for the steel is shown in Fig. 1, and the tensile properties of the steel are summarized in Table 1. The chemical compositions of the steel are shown in Table 2.

For the evaluation of the monotonic and fatigue joining strengths of the joint, two geometries of specimens (coach-peel and cross-tension) were adopted, as shown in Fig. 2. The coach-peel and cross-tension specimen geometries utilize three and four buttons, respectively, because the strength levels of specimens with one button would be too low to be controlled by a fatigue testing machine. We assume that there is no effect of multiple spot configurations on the fatigue strength. A universal testing machine (Instron 8516) was used for the clinch joining and for the tensile and fatigue testing. A set consisting of a punch with a diameter of 5.4 mm and a die with a diameter of 8.3 mm (TOX Corporation Hamburg, Germany) was used to join the specimens.

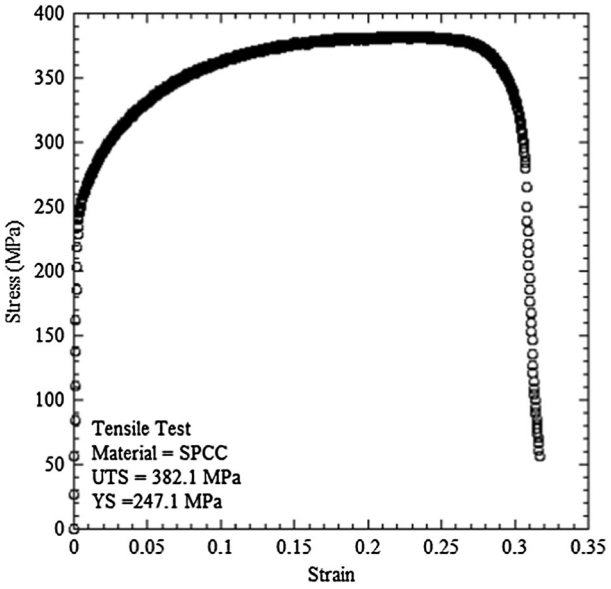

Fig. 1 Engineering stress–strain curve for the cold-rolled mild steel sheet.

Table 1 Mechanical properties of the cold-rolled mild steel

	σ_u	σ_y	E	ε_f
Material	(MPa)	(MPa)	(GPa)	(%)
SPCC	382.1	247.1	210	31.8

Table 2 Chemical compositions of the cold-rolled mild steel (wt%)

Material	C	Mn	P	S	Al	Fe
SPCC	0.04	0.25	0.01	0.005	0.05	Bal.

Tensile and fatigue tests

With regard to the monotonic joining strength of the two specimen geometries, the optimal punch force was determined to be 70 kN according to monotonic test results of specimens produced with various punch forces. Figure 3 and Table 3 show the shape and dimensions of the clinch joint specimens. The given dimensions in Table 3 are average value. The fatigue specimens, joined with the optimal punch force, were tested under a load ratio $R = (P_{min}/P_{max}) = 0.1$. The applied cyclic loading waveform was sinusoidal, and the applied frequency varied from 2 to 10 Hz, depending on load amplitude. Failure was defined as the complete separation of the specimens into two parts.

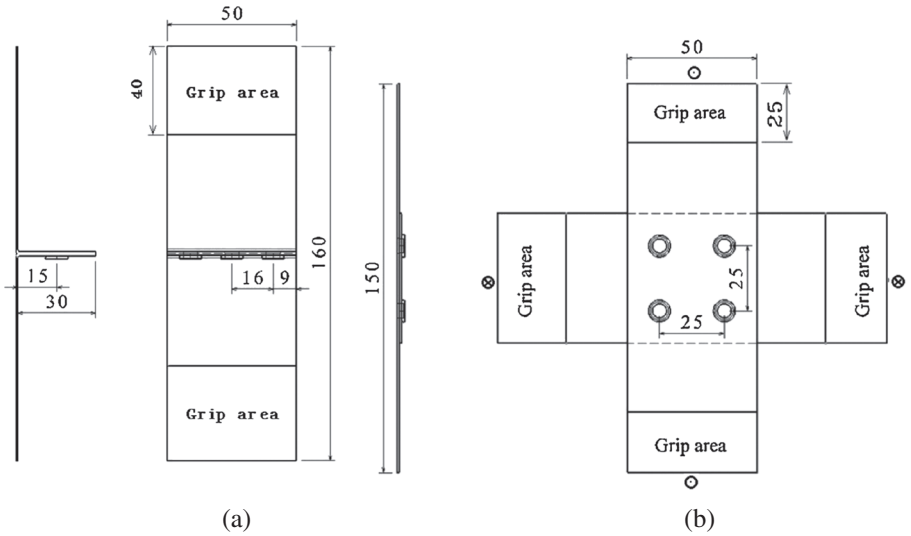

Fig. 2 Configuration of the (a) coach-peel and (b) cross-tension specimens.

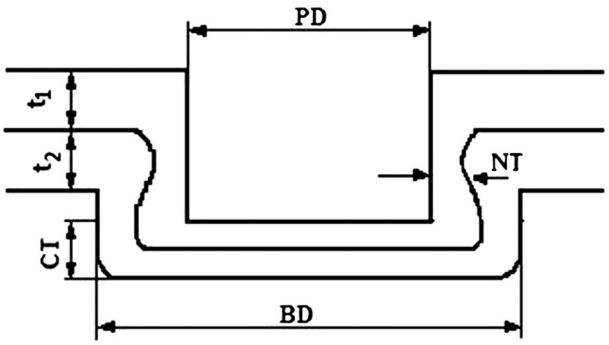

Fig. 3 Schematic depicting the dimensions of cross section of the clinch joint.

Table 3 The dimensions of the cross section of a clinch joint produced at a punching force of 70 kN

Items	Definition	Size (mm)
BD	Button diameter	8.3
CT	Cap thickness	0.4
h	Height	1.9
NT	Neck thickness	1.4
PD	Punch diameter	5.4
t_1	Punch side metal thickness	0.8
t_2	Die side metal thickness	0.8

Structural analysis of the joints

Finite element method analyses were conducted with ABAQUS (version 6.6) as the solver and HyperMesh (version 7.0) as the preprocessor and postprocessor. The coach-peel and cross-tension joints were fully modelled using linear hexahedron (eight-node) and linear prism (six-node) elements. In addition, a reduced integration scheme was used for all elements. Contact elements between the substrate faces with a friction coefficient of 0.2 were introduced by means of a master–slave technique. A penalty contact method was used to treat the contact behaviour between two faces. From an earlier test analysis of the friction coefficient when it ranged from 0.1 to 0.4, it was shown to have negligible effects. Therefore, the friction coefficient in this analysis was set to 0.2 considering the friction test results by Chowdhury *et al.*[8] Linear-elastic material model was used in the FE analysis.

EXPERIMENTAL RESULTS AND DISCUSSION

Optimal punch force for clinch joining

For coach-peel and cross-tension specimen geometries, the optimal force can differ from that of a tensile-shear specimen because of the different loading type, even if the same joining tools and the same type of sheet are used. Thus, to determine the optimal punch force for the coach-peel and cross-tension specimens in this study, a series of monotonic tests was conducted on specimens with the two geometries produced by varying the punch force. Figure 4a and b shows the maximum force for the coach-peel specimen with three buttons and for the cross-tension specimen with one button, respectively. Each data point is the average value from two specimens. The optimal punch force for both geometries was close to 70 kN, as shown in Fig. 4a and b. Therefore, all of the fatigue specimens with the coach-peel and cross-tension geometries were joined with the optimal punch force. All the coach-peel and cross-tension specimens failed in the pull-out failure mode.

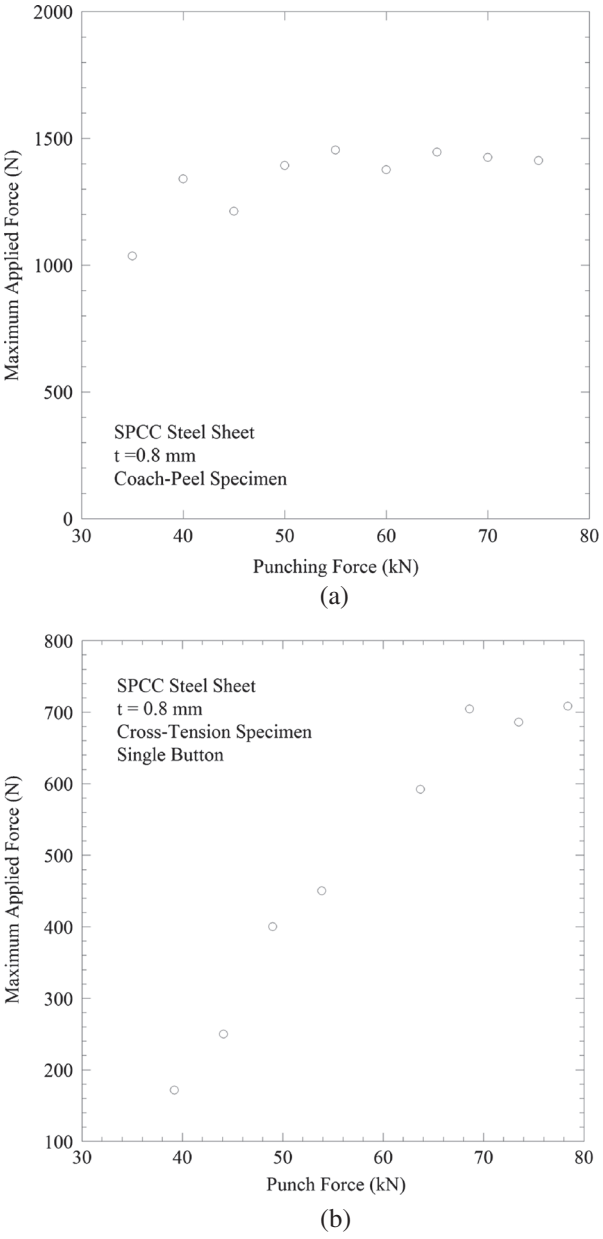

Fig. 4 Punch force against the maximum applied force for (a) the coach-peel and (b) the cross-tension specimens.

Monotonic strength of the joints

Figure 5 shows the applied load against the displacement curve of the coach-peel and cross-tension specimens produced using an optimal punch force of 70 kN. Experimental data on a tensile-shear specimen produced with the same type of sheet and under the same joining conditions[7] were included for a comparative study. The tensile-shear specimens were prepared by means of the clinch joining 30 mm by 100 mm pieces of the same SPCC steel sheet together with a 30 mm overlap.[7] Dummy plates were applied to the specimen to minimize the misalignment of the tensile-shear specimen geometry. In Fig. 5, the applied load per button for the coach-peel and cross-tension specimens was converted from the applied load divided by the number of buttons for comparative study. As shown in the figure, the coach-peel specimen exhibits the lowest strength (= 474.1 N) among the three specimen configurations because of the high stress concentrations for this loading condition. Among the three loading conditions, the tensile-shear specimen has the highest strength (= 1727.0 N). However, the coach-peel specimen shows the largest displacement at failure, compared with the other two geometries.

For the coach-peel specimen geometry, there is an initial period with high stiffness. This period corresponds to the separation between two L-type coupons with elastic deformation as load is applied. However, as the applied load gradually increased, the corner of the L-type coupon stretches, resulting in a period with low stiffness in the curve. Finally, the corner cannot stretch anymore at the maximum load, and cracking occurs at the neck of the inner button part. Consequently, there was a pull-out. However, the cross-tension specimen exhibits nearly linear deformation behaviour before final failure, which comes in the form of an abrupt button pull-out failure.

Fatigue strength of the joints

Cyclic fatigue tests were performed to investigate the fatigue strength of coach-peel and cross-tension specimens at $R = 0.1$. The fatigue life of the coach-peel and cross-tension specimens is plotted in Fig. 6 as a function of the applied load amplitude per button, including other data pertaining to the tensile-shear specimen joined by the same joining tools and with the same punching force and type of steel sheet.[7] The tensile-shear experiment was performed at a load ratio of $R = 0.1$.[7] The applied load amplitude per button for the coach-peel and cross-tension specimens was converted from the applied load amplitude divided by the number of buttons for comparative study. The fatigue strength results with the failure modes are summarized in Table 4. As shown in Fig. 6, the coach-peel specimen exhibits the lowest fatigue strength among the three specimen configurations. Among the three loading conditions, tensile-shear specimen has the highest fatigue strength. This trend is in good agreement with the static strength results and is similar to results regarding the fatigue strength of spot weld joints obtained in a previous study.[9]

From Fig. 6, for the coach-peel specimen geometry, the load amplitude per button as a function of number of cycles can be expressed as $P_{amp} = 517.3 \times N_f^{-0.19}$. The

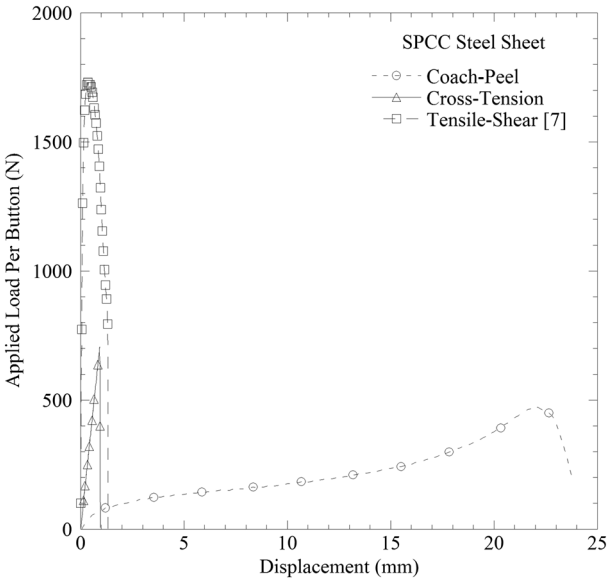

Fig. 5 Applied load per button-displacement curves of the coach-peel, cross-tension and tensile-shear[7] specimens.

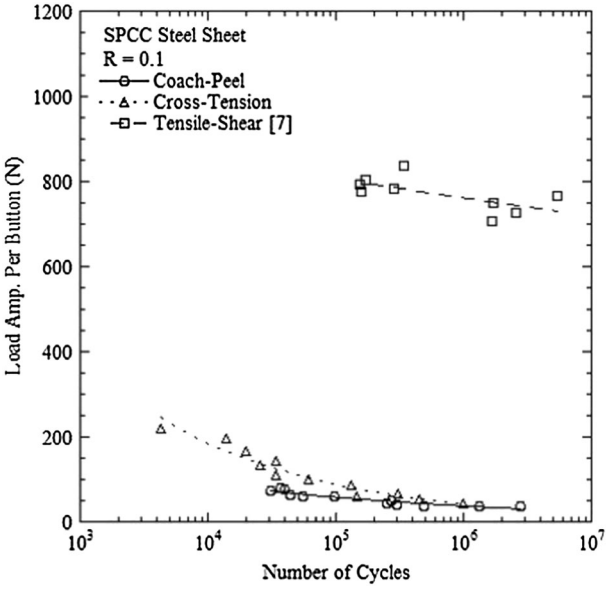

Fig. 6 Fatigue life as a function of load amplitude per button for the coach-peel and cross-tension specimens, including other data on tensile-shear specimen geometry.[7]

Table 4 Summarized fatigue testing results (P: pull-out, I: interface)

Specimen type	Maximum P (N)	N_f	Failure type
C-T	1960	4291	I + P
C-T	1764	14 036	I + P
C-T	1470	20 132	I + P
C-T	1274	33 859	I + P
C-T	1176	26 127	I + P
C-T	980	34 565	I + P
C-T	882	61 468	I + P
C-T	784	132 518	I
C-T	588	306 849	I + P
C-T	539	147 386	I
C-T	490	453 788	I
C-T	392	1 012 685	Nonfailure
C-P	539	36 887	I
C-P	509.6	39 351	I
C-P	490	30 499	I
C-P	431.2	44 381	I
C-P	411.6	97 953	I
C-P	392	55 758	I
C-P	343	273 551	I
C-P	294	253 189	I
C-P	264.6	300 693	I
C-P	254.8	493 112	I
C-P	245	2 766 202	Nonfailure
C-P	235.2	1 309 926	Nonfailure

fatigue endurance limit is 37.5 N, assuming fatigue cycles of 10^6 for an infinite life. The fatigue ratio for one button is 0.08 from 37.5/474.1 N. For the cross-tension geometry, the relationship between the load amplitude per button and number of cycles can be expressed as $P_{amp} = 3601.8 \times N_f^{-0.32}$. The fatigue ratio for one button is 0.06 from 43.3/707.9 N. The coach-peel and cross-tension specimen geometries exhibit very low fatigue ratios, considering that of the tensile-shear specimen produced under the same conditions is 0.43.[7] This indicates that the clinch joints are vulnerable to coach-peel and cross-tension loading, rather than to tensile-shear loading.

As shown in Table 4, two types of failure modes (an interface failure (I) and a pull-out failure (P)) were observed. For the coach-peel specimen geometry, all samples exhibited the pull-out failure mode under the current fatigue testing conditions, as shown in Fig. 7a. For the cross-tension specimen geometry, a mixed (pull-out and interface) failure mode was noted in low and intermediate cycle regions, as shown in Fig. 7b. However, the interface failure mode tended to occur, in the high cycle region ($N_f > 10^5$). It appears that crack initiated at the neck of inner button part and propagated through the sheet thickness along the neck.

Figure 8a, 8b and 8c shows the interface fracture surfaces of the coach-peel sample when $P_{max} = 539$ N. A crack initiated near point 'a' and propagated from the bottom of Fig. 8a, and after which, it moved to point 'b'. It propagated diagonally from the lower-left corner

(a)

(b)

Fig. 7 Fatigue fractured specimens in (a) interface failure mode for the coach-peel sample at $P_{max} = 539$ N and (b) mixed (pull-out and interface) failure mode for the cross-tension sample at $P_{max} = 539$ N.

in Fig. 8b and then reached point 'c'. It propagated horizontally from left to right in Fig. 8c and finally fractured near point 'c'. Figure 8 shows many striations, indicating that the striation space corresponds to the crack growth rate. The average striation spaces at 'a', 'b' and 'c' are approximately 0.7, 0.6 and 1.0 μm, respectively. Normally, the crack growth rate increases as crack length increases. Thus, the average striation space is expected to increase. At present, it is not clear that the striation space decreases near 'b'. This may be partially due to change in loading mode from tensile mode to shearing or mixed (shearing + tensile) loading. The shearing component leads to the retardation of crack growth, causing roughness-induced crack closure. The distance from 'a' to 'c' is 8 mm. The number of crack propagation cycles from crack initiation to failure can be predicted to be approximately 10 400 cycles

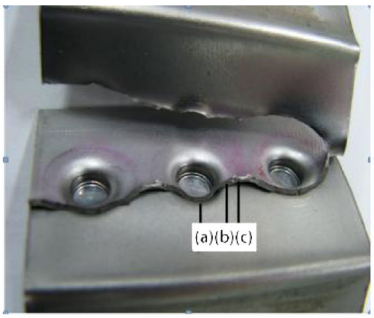

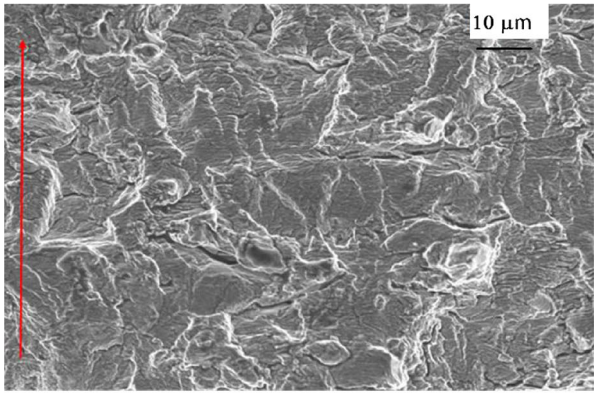

(a)

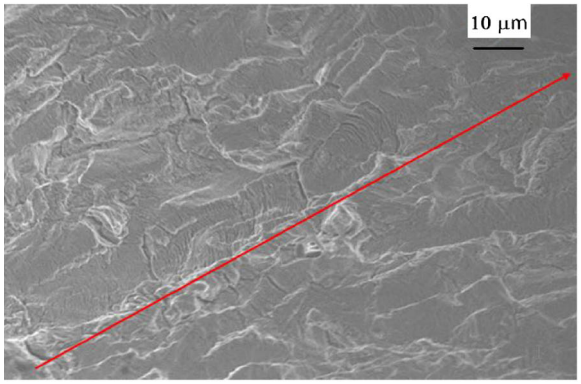

(b)

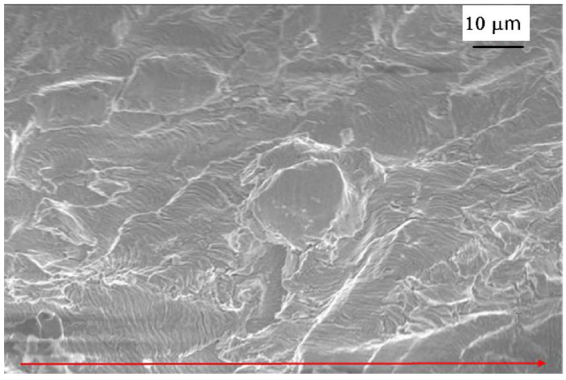

(c)

Fig. 8 Fatigue fractured surfaces at (a), (b) and (c) locations of the coach-peel sample at P_{max} = 539 N.

(= 8000/0.77 μm), assuming that the average crack growth rate from 'a' to 'c' is 0.77 μm. The number of cycles to failure of the sample at P_{max} = 539 N is 36 887 from Table 4.

Structural analysis of the joints

The structural analysis results of the cross-tension specimen at P = 176.4 N, corresponding to a fatigue endurance limit value at R = 0.1, are shown in Fig. 9. The FE results show that the stress values in the clinch joint are highly complex. The maximum von Mises stress occurs on the outer convex edge of a button on the lower sheet neck, as shown in Fig. 9a. The maximum principal stress occurs on the outer convex edge of a button of the upper sheet neck where the upper and lower sheets connect, as shown in Fig. 9b. This site coincides with the location where cracking was observed, as shown in Fig. 9c. A crack is expected to initiate at the button's outer surface on the upper sheet neck and propagate into the button's inner surface.

The maximum von Mises stress of 784.0 MPa and the maximum principal stress of 642.0 MPa in Fig. 9a and b are higher than the ultimate tensile strength of the SPCC sheet (= 382.2 MPa). This implies that the true tensile strength of the neck is significantly increased through cold clinch joining. This concept can be partially proved by considering the maximum true tensile strength of 435 MPa for this steel sheet.[7] We also measured micro-Vickers hardness of the clinch joint to verify our argument. From this test result, the hardness values of the neck and undeformed section are 185 and 89 H_v. This result strongly supports our argument. Also, compressive residual stresses produced by clinch joining of the joint may have an additional beneficial effect on the fatigue strength of the joints.

Figure 10 shows the stress distributions of the coach-peel specimen at P = 110.3 N, corresponding to a fatigue endurance limit value based on fatigue cycles of 10^6 for an infinite life. The maximum von Mises stress of 509.1 MPa is located on the button's inner surface of the upper sheet in Fig. 10a. Figure 10b also shows that the maximum principal stress of 575.5 MPa is located on the outer convex edge of a button on the upper sheet neck where the upper and lower sheets connect. The maximum principal stress and von Mises stress positions on the upper sheet correspond to the critical crack initiation location, where cracking occurred on the neck, similar to the pattern shown in Fig. 9c. This indicates that the maximum principal stress or/and von Mises stress can be a parameter to predict the fatigue life of a clinch joint. The values of the maximum von Mises and principal stress amplitude corresponding to the fatigue endurance limit value at R = 0.1 are much higher than the Ultimate Tensile Strength (UTS) of the sheet (= 382 MPa).

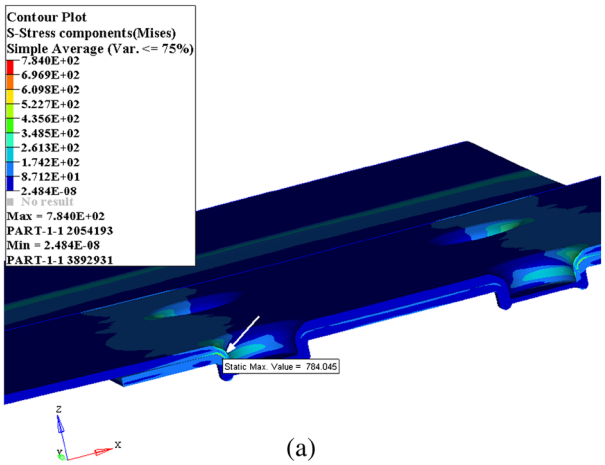

Fig. 9 (a) Von Mises stress distribution, (b) the maximum principal stress distribution and (c) fatigue fractured cross section of the cross-tension specimen under an applied load amplitude of 173.2 N.

The structural analysis results of the tensile-shear specimen when P = 705.6 N, corresponding to the fatigue endurance limit value at R = 0.1, are shown in Fig. 11.

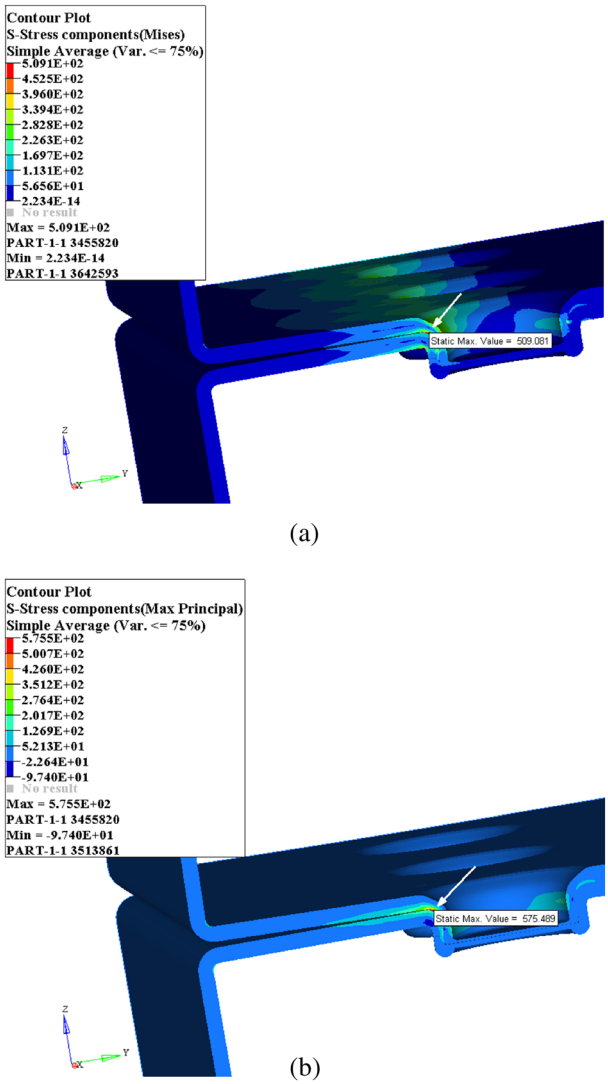

Fig. 10 (a) Von Mises stress distribution and (b) maximum principal stress distribution of the coach-peel specimen under an applied load amplitude of 110.3 N.

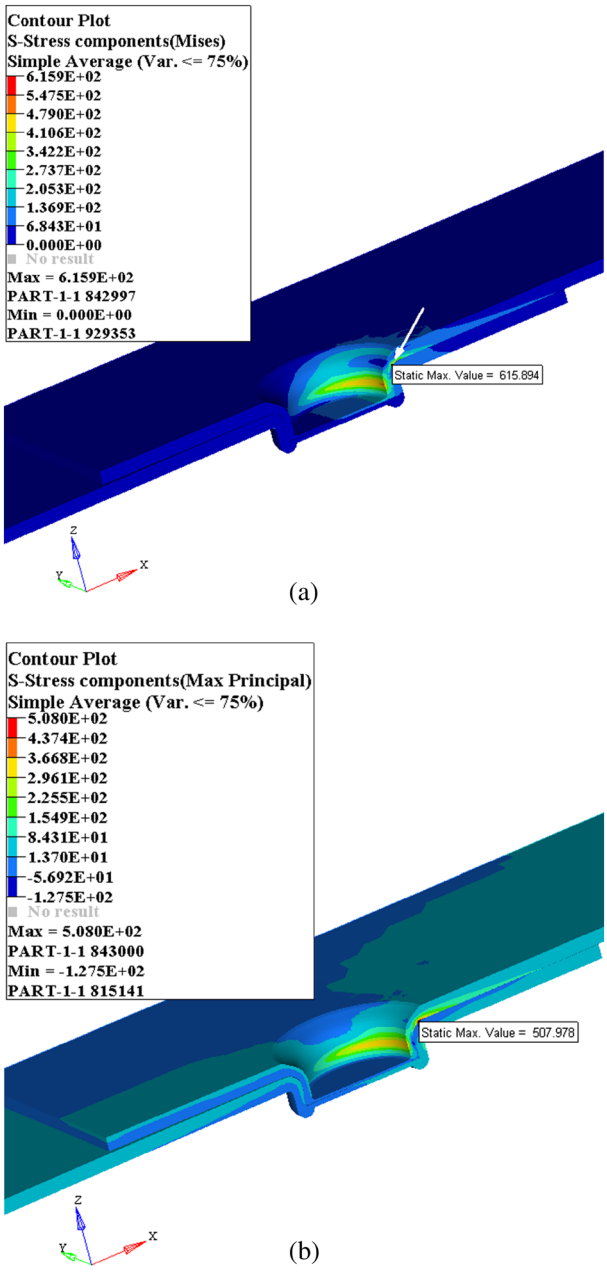

Fig. 11 (a) Von Mises stress distribution and (b) the maximum principal stress distribution of the tensile-shear specimen under an applied load amplitude of 705.6 N.

The maximum von Mises stress of 615.9 MPa occurs on the inner concave surface of a button on the upper sheet neck, as shown in Fig. 11a. The maximum principal stress of 508.0 MPa occurs on the outer convex surface of a button on the upper sheet neck, as shown in Fig. 11b. The maximum von Mises stress is much higher than the true tensile strength of 435 MPa.[7] Compressive residual stresses produced by clinch joining on the joint can have an additional beneficial effect on the fatigue strength of the joints. Further study is needed with regard to the distribution and magnitude of the residual stress on the joints.

Fatigue life prediction

The applied load amplitude cannot correlate the fatigue life of different specimen geometries, such as the cross-tension, coach-peel and tensile-shear geometries. Therefore, the fatigue life must be predicted, adopting other parameters that can incorporate various geometric factors. In this study, we select the von Mises effective stress, the maximum principal stress and the Smith–Watson–Topper (SWT) fatigue parameter[9] to predict the experimental fatigue life.

The von Mises effective stress is generally effective when used to predict the fatigue failure lifetimes of components with complicated geometries. The

maximum principal stress can be utilized to evaluate the fatigue strength of clinch joints, because FEM analysis results reveal that the regions with the maximum principal stress coincide with crack initiation sites in fatigue failed specimens with cross-tension and coach-peel geometries. The SWT parameter is also used, because the stress state at the clinch joint is normally multiaxial. The SWT[10] relationship was adopted to evaluate the fatigue life of the clinch joints, as shown in the succeeding text.

$$\sigma_1^{\max}\frac{\Delta\varepsilon_1}{2}=\frac{\left(\sigma_f'\right)^2}{E}\left(2N_f\right)^{2b}+\sigma_f'\varepsilon_f'\left(2N_f\right)^{b\ +\ c} \quad (1)$$

Here, $\Delta\varepsilon_1/2$ is the maximum principal strain amplitude and $\sigma_1^{\max}$ is the maximum stress on the $\Delta\varepsilon_1$ plane. In addition, σ_f' and ε_f' correspond to the fatigue strength and the fatigue ductility coefficient, respectively, and b and c are the fatigue strength and the fatigue ductility exponents, respectively. Finally, E is the elastic modulus and $2N_f$ is the fatigue life. Thus, the SWT fatigue parameter of the left term in Eq. (1) can be adopted to evaluate the fatigue life of clinch joints.

Applied load amplitudes are converted into the form of effective stress against fatigue life (Fig. 12), maximum principal stress against fatigue life (Fig. 13) and SWT fatigue parameter against fatigue life (Fig. 14). In these figures, we add the scatter index T, which quantifies the width of the scatter band included between the 10% and 90% probabilities of survival curves. The effective stress ($R\approx0.87$) and maximum principal stress ($R\approx0.89$) correlate satisfactorily the fatigue life for the clinch joints, as shown in Figs. 12 and 13. From Fig. 14, however, the SWT parameter ($R\approx0.93$) shows a better correlation with experimental data, including data for the tensile-shear specimen geometry,[7] compared with data based on effective stress and the maximum principal stress. Therefore, the SWT parameter can predict appropriately the current experimental fatigue lifetimes, including the data for the tensile-shear specimen geometry.[7] The SWT parameter can be expressed as $SWT=605.2N_f^{-0.437}$.

The clinch joint is expected to undergo significant hardening during cold clinch joining, which was accompanied by a considerable increase in the cyclic yield strength under cyclic loading. Thus, there is a high probability of appearance of material property mismatching, as determined under cyclic and static loading conditions. This concept is verified by an increase in hardness of the joint from 89 H_v for undeformed section to 189 H_v for the neck. Therefore, it is desirable to use cyclic stress–strain curve, rather than the true stress–strain curve, for a structural analysis of a joint. However, it may be very complicated to adopt the cyclic stress–strain curve for structural analysis of a joint even under a multiaxial stress condition. There may be more error in material deformation behaviour if we adopt nonlinear model in place of a linear-elastic material model. Thus, a linear-elastic material model appears to be more feasible. Accordingly, we verify this possibility by adopting nonlinear kinematic hardening elastic–plastic material model. It was found that maximum principal stress and effective

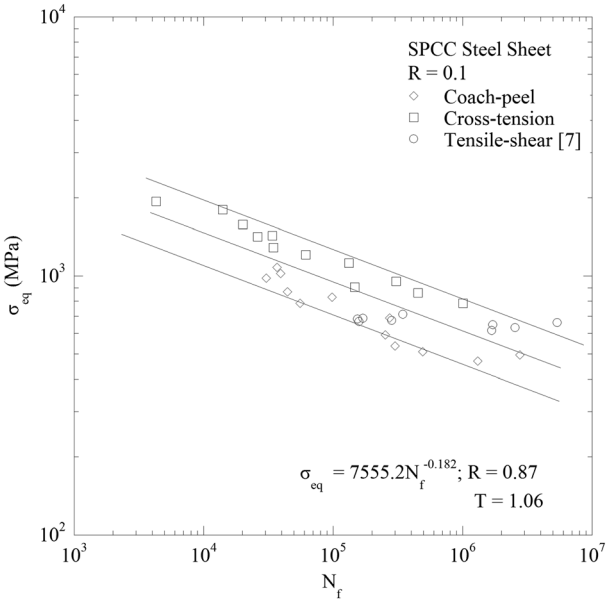

Fig. 12 Fatigue life as a function of effective stress amplitude for the coach-peel and cross-tension specimens, including other data on the tensile-shear specimens.[7]

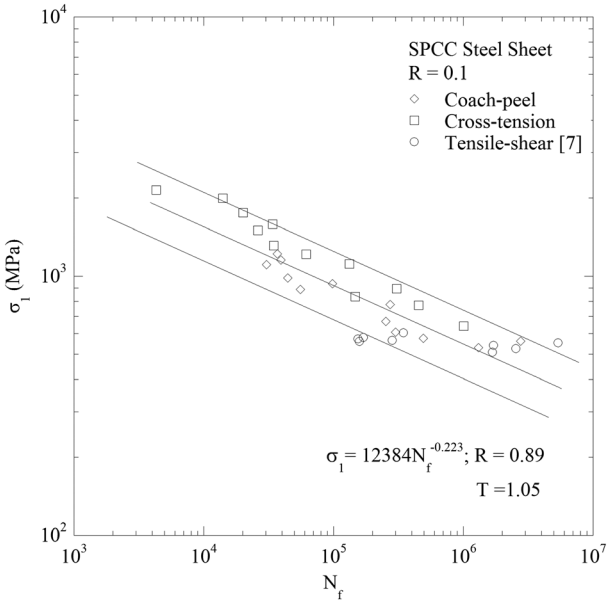

Fig. 13 Fatigue life as a function of maximum principal stress amplitude for the coach-peel and cross-tension specimens, including other data on the tensile-shear specimens.[7]

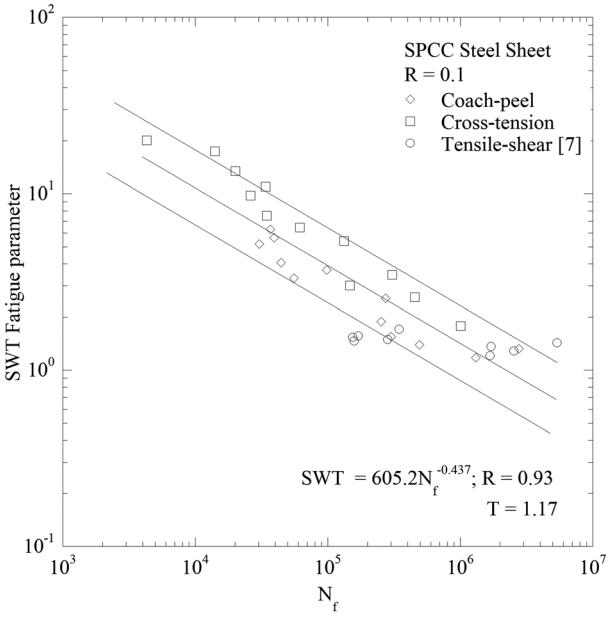

Fig. 14 Fatigue life as a function of Smith–Watson–Topper parameter for the coach-peel and cross-tension specimens, including other data on the tensile-shear specimens.[7]

stress show worse correlation with the experimental fatigue life with correlation factor R of 0.84 and 0.78, respectively, compared with the results from a linear-elastic material model. The SWT parameter ($R \approx 0.93$) still exhibits a good correlation with the experimental fatigue life. However, further study is needed to verify these parameters to correlate the fatigue life of joints with different sheet materials, loading-type geometries, dissimilar materials combinations and other factors.

CONCLUSION

Monotonic tensile and fatigue tests were conducted using coach-peel and cross-tension specimens to evaluate the

fatigue strength of clinch joint specimens with a steel sheet. A linear-elastic material model was used in the FE analysis. The optimal punch force was found to be 70 kN with the current sheet thickness and the joining tool.

The monotonic experimental results reveal that the coach-peel specimen exhibits the lowest strength among the three specimen configurations. The coach-peel and cross-tension specimen geometries exhibit very low ratios of fatigue endurance limit to the monotonic strength, compared with that of the tensile-shear specimen. This indicates that clinch joints are vulnerable to coach-peel and cross-tension loading, rather than to tensile-shear loading.

The FEM analysis shows that crack initiation sites coincide with the locations that have the maximum principal stress for cross-tension geometry. The maximum principal stresses at the fatigue endurance limit value when $R = 0.1$ are much higher than the engineering tensile strength of the steel for the three specimen geometries. This suggests that the strength of the neck is increased significantly during cold clinch joining. Also, compressive residual stresses produced by clinch joining on the joint may have an additional beneficial effect on the fatigue strength of the joints.

Compared with effective stress and maximum principal stress, the SWT fatigue parameter can predict appropriately the experimental fatigue lifetimes, including data pertaining to the tensile-shear specimen geometry. The SWT parameter can be expressed as $SWT = 605.2N_f^{-0.437}$. For coach-peel specimen geometry, all the samples exhibit pull-out failure mode in the fatigue testing range. However, for the cross-tension specimen geometry, mixed (pull-out and interface) failure mode occurred in low and intermediate cycle regions. In contrast, in the high cycle region ($N_f > 10^5$), the interface failure mode tends to occur.

Acknowledgement

This study was supported by Research Programme funded by the Seoul National University of Science and Technology.

REFERENCES

1 Sawhill, J. M., Sawdon, S. E. (1983) A new mechanical joining technique for steel compared with spot welding. *SAE paper*. 830128, 1–12.
2 Davies, R., Pedreschi, R. Shiha, B. P. (1996) The shear behavior of press-joining in cold-formed steel structures. *Thin-Walled Struct.*, **25**, 153–170.
3 Varis, J. P., Lepisto, J. (2003) A simple testing-based procedure and simulation of the clinching process using finite element analysis for establishing clinching parameters. *Thin-Walled Struct.*, **41**, 691–709.
4 de Paula, A. A., Aguilar, M. T. P., Pertence, A. E. M., Cetlin, P. R. (2007) Finite element simulations of the clinch joining of metallic sheets. *J. Mater. Process. Tech.*, **182**, 352–357.
5 Hamel, V., Roelandt, J. M., Gacel, J. N., Schmit, F. (2000) Finite element modeling of clinch forming with automatic remeshing. *Comput. Struct.*, **77**, 185–200.
6 Carboni, M., Beretta, S., Monno, M. (2006) Fatigue behavior of tensile-shear loaded clinched joints. *Eng. Fract. Mech.*, **73**, 178–190.
7 Kim, H. K. (2013) Fatigue strength evaluation of the clinched lap joints of a cold rolled mild steel sheet. *J. Mat. Eng. Perform.*, **22**, 294–299.
8 Chowdhury, M. A., Nuruzzaman, D. M., Roy, B. K., Islam, A., Hossain, Z., Hasan, M. R. (2013) Experimental investigation of friction coefficient and wear rate of stainless steel 202 sliding against Smooth and rough stainless steel 304 counter-faces. *Fric. Wear Res.*, **1**, 34–41.
9 Kim, D. H., Kim, H. K. (2009) Fatigue strength evaluation of cross-tension spot weld joints of cold rolled mild steel sheet. *Mater. Design.*, **30**, 3286–3290.
10 Smith, R. N., Watson, P., Topper, T. H. (1970) A stress–strain function for the fatigue of metals. *J. Mater.*, **5**, 767–778.